Electronic Structure Calculations on the Reaction of Vinyl Radical with Nitric Oxide

Raman Sumathi

Lehrstuhl für Theoretische Chemie, Universität Bonn, Wegelerstrasse 12, D-53115 Bonn, Germany

Hue Minh Thi Nguyen

Faculty of Chemistry, College of Education, Vietnam National University, Hanoi, Vietnam

Minh Tho Nguyen* and Jozef Peeters

Department of Chemistry, University of Leuven, Celestijnenlaan 200F, B-3001 Leuven, Belgium

Received: September 14, 1999; In Final Form: November 2, 1999

The potential energy surface of the [C_2,H_3,N,O] system in its electronic singlet ground state has been investigated using second-order Möller Plesset perturbation theory (MP2) and coupled-cluster theory CCSD(T) with the 6-311++G(d,p) basis set. Twenty-six (26) reactive intermediates relevant to the C_2H_3 + NO reaction channel have been identified. Methyl isocyanate **19** is calculated to be the most stable isomer. Two mechanisms (mechanisms **A** and **B**) are found to operate competitively toward CH_2O formation, and they include reactive intermediates such as *trans*-nitrosoethylene **1**, *cis*-nitrosoethylene **2**, cyanomethanol **13**, isocyanomethanol **14**, and the cyclic oxazete **3**. While the rate-limiting step in mechanism A is the decomposition of the cyclic oxazete **3**, in mechanism B it corresponds to a 1,3-H shift in the *trans*-nitrosoethylene **1**. The potential energies of both these critical transition structures are somewhat higher than the energy of the reactants C_2H_3 + NO, which explains the nonobservation of CH_2O in the low-temperature pyrolysis of acetylene in the presence of NO. At low temperatures, the stabilized nitrosoethylenes **1** and **2** will be the dominant products, together with the cyclic compounds **3** and to a lesser extent, also **11**. H_2CO + HCN is predicted to be the predominant product at high temperatures. Conversion of NO to CO is kinetically unfavorable due to the high barrier involved in the isomerization of fulminate **15** to isofulminate **16**. The most favorable mode of [2+2] cycloaddition between CH_2O and HCN is the one wherein the carbon of the carbonyl group adds on to the nitrogen end of the cyanide.

Introduction

The pyrolysis of acetylene has been extensively studied over the past sixty years. The salient aspects of this pyrolysis are (a) from 400 to 700 °C, the reaction is an auto-catalyzed radical chain polymerization,[1−3] producing very few species smaller than C_4H_4; (b) the overall reaction rate is close to second order in acetylene concentration;[1−5] (c) there is a distinct and reproducible induction period, which decreases with increasing temperature and increasing acetylene concentration;[1,2,5] (d) small amounts of NO (0.1−2%) inhibit the reaction;[1,2,6,7,8a] (e) during the NO inhibited reaction, the NO is very slowly consumed together with some acetylene, after which the reaction proceeds with its normal rate;[1,2] and (f) above 2000 K, NO was found[8b] to have no effect on the pyrolysis of acetylene. Although the inhibiting effect by nitric oxide on the acetylene pyrolysis is of interest in combustion chemistry, only a few studies have been reported on the kinetics or the chemistry of the NO−C_2H_2 system.

Frank-Kamenetsky[1] studied this reaction over the range of 673−973 K and reported that the rate of loss of NO during the induction period is very slow but is second order in C_2H_2 and virtually independent of the NO concentration. Based on his experimental findings, he proposed a kinetic scheme wherein NO disappears in a bimolecular reaction with a radical produced in the system during the bimolecular reactions of C_2H_2. More specifically, according to his scheme, NO radicals are not involved in the initiation step. Low-temperature studies (625−745 K) were made by Silcocks.[2] He reported a first-order dependence of the NO loss rate on C_2H_2 and a fractional order dependence (0.24) on NO. The third study was the single pulse shock tube study by Ogura[8] at about 2.5 atm over the temperature range of 1100−1650 K. This author observed a ≈ 1:1 production of CO and HCN which accounted for about 90% of the NO consumed. CO and HCN were formed at about 0.15 to 0.50 of the rate of formation of the major product, vinylacetylene, in the second-order process from C_2H_2 and NO. The radical chain mechanism was reported to be initiated by the bimolecular reaction of acetylene, viz.,

$$2C_2H_2 \rightarrow C_4H_3 + H$$

yielding 1-ethynyl and 2-ethynylvinyl radicals as the chain carriers. However, the experimental observations of Ogura led Benson[9] to suggest a radical chain mechanism as follows:

$$NO + C_2H_2 \xrightarrow{i} H + CO + HCN$$

$$H + C_2H_2 \overset{1}{\rightleftharpoons} C_2H_3(V^\bullet)$$

* Author for correspondence. E-mail: minh.nguyen@chem.kuleuven.ac.be.

10.1021/jp993274l CCC: $19.00
Published on Web 02/15/2000

$$V^{\bullet} + C_2H_2 \overset{2}{\rightleftharpoons} CH_2{=}CH{-}CH{=}CH^{\bullet} \overset{2H}{\rightleftharpoons} CH_2{=}CH{-}C{\equiv}CH + H$$

$$V^{\bullet} + NO \overset{t}{\rightleftharpoons} C_2H_3NO \rightarrow CH_2O + HCN$$

in which chains are both started and stopped by NO. The initiation step is not a direct bimolecular reaction and could proceed via one or more intermediates, and therefore it was difficult to select the rate-determining step for the overall path. In our recent ab initio study,[10] we characterized the potential energy surface (PES) of the [C_2,H_2,N,O] system and established the main mechanism for the formation of HCO + HCN in the reactions of C_2H_2 + NO. However, as commented by Kiefer,[11] it is essential to derive an understanding about the radical termination reaction viz., C_2H_3 + NO, to understand what actually happens during the pyrolysis of acetylene in the presence of nitric oxide. Furthermore, a knowledge about this reaction is equally important to understand the chemistry of the fuel-rich reburn zone with ethane,[12a] ethene,[12b] and propene[12c] as the reburn fuels.

Sherwood and Gunning[13,14] produced vinyl radical at 300 K by the Hg-sensitized photolysis of C_2H_2 with added NO and showed that HCN, CH_2O, propynal, and CO (1:0.4:0.5:0.1) were the major products. The HCN quantum yields were pressure-sensitive and reached a maximum at about 7 torr, suggesting the quenching of the vibrationally excited C_2H_3NO species. However, the mechanism for the formation of CH_2O in the reaction of vinyl radical with NO is not yet clear. Furthermore, in addition to CH_2O + HCN, one can expect other products viz., CH_2O + HNC, CO + CH_2NH, CO + H_2NCH. Of the latter, the CO + CH_2NH fragments are thermochemically more stable than H_2CO + HCN. To our knowledge, the existing theoretical works[15] on [C_2,H_3,N,O] are largely confined to the determination of the equilibrium structure of the various isomers of [C_2,H_3,N,O] and often only at the Hartree−Fock level of characterization. The only previous theoretical study on the decomposition reaction of nitrosoethylene to CH_2O + HCN was by Ugalde[16a] and was done at the Hartree−Fock level of theory. Hence, the main goal of the present work is to map out the global features of the singlet PES of [C_2,H_3,N,O] and to investigate all isomerization and fragmentation pathways. After a brief outline of the calculation methods, we present the results of our investigation and subsequently discuss the various possible channels and mechanisms for HCN and CO formation.

Methods of Calculation

Ab initio molecular orbital calculations were carried out using the Gaussian 94 set of programs.[17] All the geometries on the PES have been optimized without any symmetry constraints at the second-order Moller Plesset perturbation level by including all electrons for the correlation correction and by using the standard 6-31G(d,p) and 6-311++G(d,p) basis sets. Vibrational frequencies, calculated at the MP2/6-31G(d,p) level, have been used for characterizing the stationary points as equilibrium and transition structures and for estimating zero-point energy (ZPE) corrections. The identity of each first-order stationary point is determined by intrinsic reaction coordinate (IRC) calculations. To calibrate the relative energies, single-point electronic energies using coupled-cluster theory, which includes all single and double excitations plus perturbative corrections for triples, CCSD(T)/6-311++G(d,p), have also been computed using MP2/6-311++G(d,p) optimized geometries for a number of structures. Due to the large number of reaction pathways considered and since the higher level CCSD(T)/6-311++G(d,p)//MP2/6-311++G(d,p) results compare quite well with MP2/6-311++G(d,p) results (as shown in Table 1 and Figure 4), the MP2-relative energies will be employed for the discussion. Therefore, we put less importance on the quantitative description of the PES but rather focus on its global shape in order to understand the mechanism of the reaction under consideration.

TABLE 1: CCSD(T)/6-311++G(d,p)//MP2(fu)/6-311++G(d,p) Computed Heats of Reaction and Activation Barriers for the Various Processes on [C_2,H_3,N,O] PES Relevant to the C_2H_3 + NO Reaction

reaction	ΔE	E_a	reaction	ΔE	E_a
1 → **2**	3.6	7.4	**2** → **3**	0.9	35.3
3 → **27**	−43.7	47.7	**3** → **4**	37.9	71.2
5 → **27**	−12.7	53.4	**5** → **6**	41.0	67.1
6 → **7**	−22.5	14.2	**7** → **8**	−32.5	23.4
8 → **9**	24.3	71.3	**8** → **29**	−4.8	85.8
8 → **30**	35.0	78.5	**7** → **29**	−42.7	25.3
7 → **27**	−31.2	60.9	**8** → **25**	52.6	82.5
7 → **23**	7.9	45.6	**1** → **11**	35.5	47.9
11 → **31**	17.5	56.4	**1** → **12**	3.0	62.3
13 → **14**	16.5	50.9	**13** → **28**	26.5	65.5
14 → **27**	−5.0	49.3	**1** → **15**	−5.4	65.8
12 → **15**	−8.4	61.2	**15** → **16**	24.2	97.2
16 → **17**	−56.6	27.4	**17** → **19**	−25.1	58.0
19 → **20**	19.1	66.0	**20** → **29**	−6.8	69.1
20 → **21**	35.2	73.5	**21** → **22**	−9.8	26.6
23 → **24**	−16.5	20.8			

Results and Discussion

Nearly 39 bound, topologically different C_2H_3NO isomers have been identified, and they include open-chain (around 15), cyclic (6 three-membered rings, 5 four-membered rings, and 1 bicylic species), and electron-deficient (6 carbenes and 1 nitrene) structures. However, 13 of these isomers are not really relevant in the study of the reaction between vinyl radical and NO and hence will not be included hereafter for discussion. The optimized structures of these isomers are shown in Figures 1−3 along with their relative energy with respect to *trans*-nitrosoethylene **1**. The reactions investigated in this study are shown in Scheme 1 and are further categorized into five different pathways, i.e., **A**, **A′**, **B**, **C**, and **D**. Pathway **D** includes rearrangements to carbenes and the cyclization of carbenes into three-membered rings. A schematic representation of the potential energy surface (PES) for the C_2H_3 + NO reaction is presented in Figure 4. Each of the stationary points in Figure 4 and Scheme 1 is labeled with a number in order to facilitate the discussion. While the various isomers of the [C_2,H_3,N,O] system are associated with numbers ***i*** from **1** to **26**, the various product limits viz., H_2CO + HCN, H_2CO + HNC, CO + CH_2NH, CO + $CHNH_2$, and C_2H_3 + NO are labeled, respectively, from **27** to **31**. Figure 5 displays the MP2 optimized transition-state structures on the C_2H_3 + NO PES leading to H_2CO + HX (X = −CN, −NC) products as per mechanisms **A** and **B**. Figure 6 shows the transition structures involved in mechanisms **C**, leading to the CO product, and **D**, to cyclic intermediates. The transition structures associated with mechanism **A′** are displayed in Figure 7. In Figures 1−3 and 5−7, bond lengths are given in angstroms and bond angles in degrees. As for a convention, **i/j** stands for a transition structure connecting the equilibrium structures **i** and **j**. The harmonic vibrational frequencies of the various [C_2,H_3,N,O] isomers and transition structures for isomerization and dissociation are available as supporting material. Table 1 records the relative energies

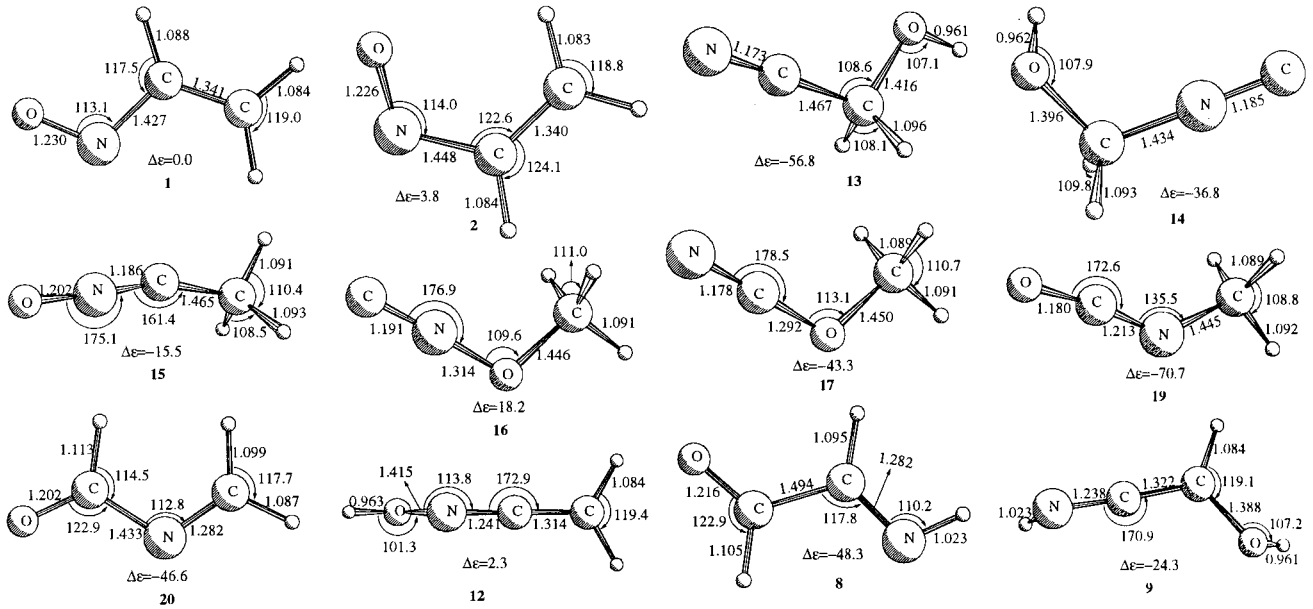

Figure 1. MP2/6-311++G(d,p) optimized geometries of the open-chain intermediates relevant to C_2H_3 + NO reaction in [C_2,H_3,N,O] PES. Bond lengths are given in Å and bond angles in degrees.

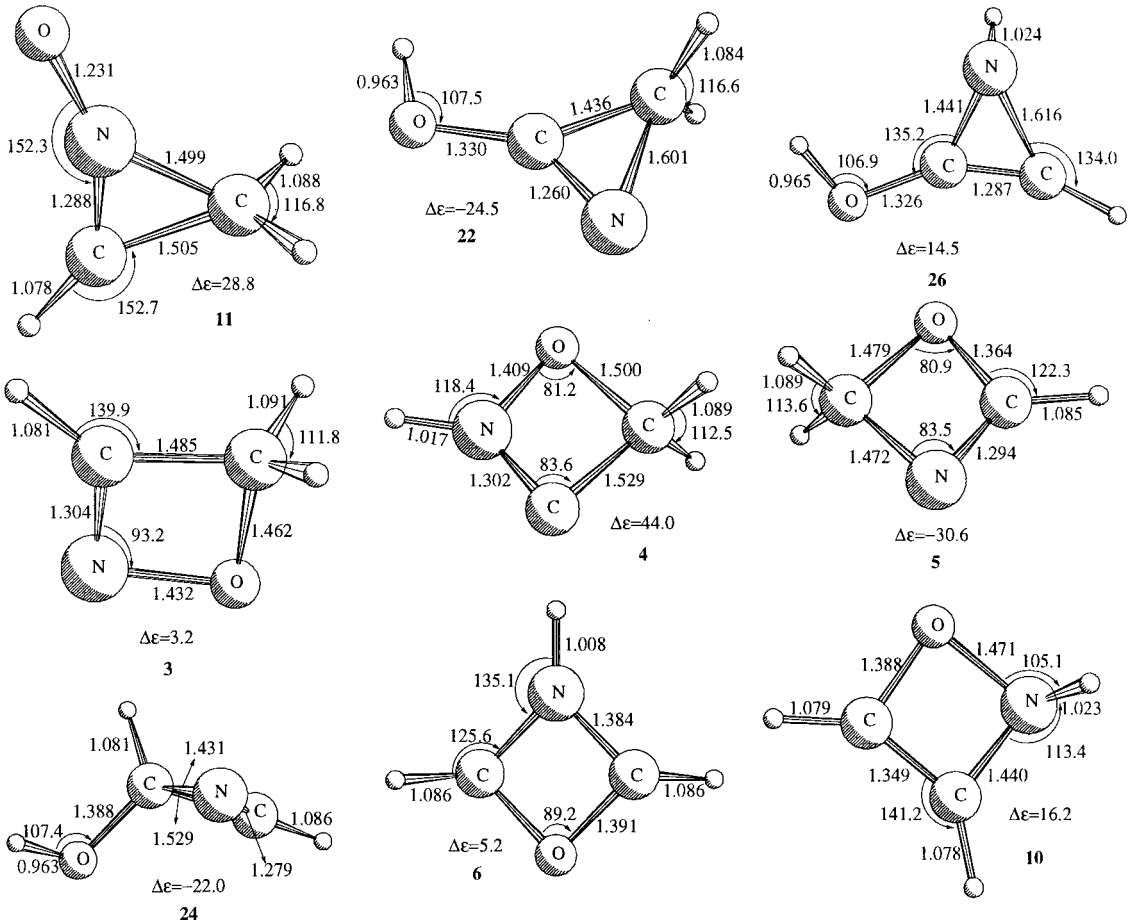

Figure 2. MP2/6-311++G(d,p) optimized geometries of the cyclic intermediates relevant to C_2H_3 + NO reaction in [C_2,H_3,N,O] PES. Bond lengths are given in Å and bond angles in degrees.

obtained using single-point CCSD(T)/6-311++G(d,p) calculations on the MP2 geometries. In general, the magnitude of the relative energies are not significantly modified in going from MP2 to CCSD(T). As mentioned above, for the sake of consistency, the values quoted hereafter refer to the MP2 results.

Equilibrium Structures. The combination of the NO radical with the vinyl radicals proceeds without a barrier and leads to a planar *trans*-nitrosoethylene, $H_2C{=}CH{-}NO$ **1** (ONCC 180°) or to *cis*-nitrosoethylene **2** as the initially formed energized adduct. The energy difference between the reactant limit, C_2H_3 + NO, and the adduct **1** is about 54.0 kcal/mol. It is appropriate to mention that both C_2H_3 and NO radicals have a degenerate ground state and hence their energy cannot be obtained exactly by the single configuration approach that we have employed

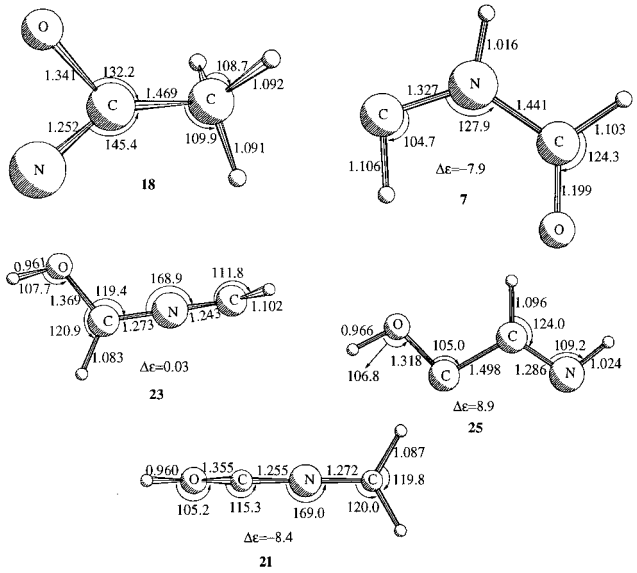

Figure 3. MP2/6-311++G(d,p) optimized geometries of the electron-deficient intermediates relevant to C_2H_3 + NO reaction in [C_2,H_3,N,O] PES. Bond lengths are given in Å and bond angles in degrees.

here. Twelve open-chain isomers of [C_2,H_3,N,O], as shown in Figure 1, have been found on the singlet MP2 potential energy surface. The various open-chain isomers correspond to (i) nitroso-substituted ethylenes (**1** and **2**), (ii) cyano- (**13**) and isocyano- (**14**) substituted methanol, (iii) C-formyl (**8**) and N-formyl (**20**) substituted imine, (iv) methyl-substituted [CNO] functionalities (**15**, **16**, **17**, and **19**), (v) hydroxy-keteneimine (**9**), and (vi) substituted oximes (**12**). Note that an earlier theoretical study[16b] using HF and MP2/6-31G(d) calculations considered only five isomers. From the present study, the most stable isomer is computed to be methyl isocyanate, CH_3 NCO (**19**), which lies approximately 70.7 kcal/mol below the initially formed *trans*-nitrosoethylene, $H_2C{=}CH{-}NO$ (**1**). This is in accordance with the earlier finding[18] that the isocyanic acid, HNCO, is the most stable structure among the isomers of [H,C,N,O]. Methyl cyanate **17**, lies by 27.4 kcal/mol higher than CH_3NCO. The relative stability of methyl substituted cyanate, isocyanate, fulminate, and isofulminate is found to be $CH_3{-}$NCO **19** > $CH_3{-}$OCN **17** > $CH_3{-}$CNO **15** > $CH_3{-}$ONC **16**.

The isomers of substituted methanol, cyanomethanol (**13**), and isocyanomethanol (**14**) are found to be more stable than the fulminates (**15**). As can be seen from Figure 1, the relative energy ordering among the open chain isomers is $CH_3{-}$NCO **19** < CH_2(OH)CN **13** < HC(O)CHNH **8** < HC(O)N$=CH_2$ **20** < $CH_3{-}$OCN **17** < CH_2(OH)NC **14** < CH(OH)$=$C$=$NH **9** < $CH_3{-}$CNO **15** < *trans*-C_2H_3NO **1** < $CH_2{=}C{=}$NOH **12** < *cis*-C_2H_3NO **2** < $CH_3{-}$ONC **16**. Since all these isomers lie energetically below the initial reactant limit, C_2H_3 + NO, it is essential to consider the dissociation and decomposition channels arising from these isomers.

The well-known[19] unimolecular reactions of nitrosoalkenes is the intramolecular cyclization leading to the four-membered oxazetes, which in turn can decompose to form the carbonyl compound and nitrile oxide. We have optimized the structure of both 1,2- and 1,3-oxazetes (**3** and **5**), of which the latter **5** is found to be more stable than **3** as well as the nitrosoethylene **1** (Figure 4a). Besides oxazetes, a few other four-membered ring isomers of [C_2,H_3,N,O] have been identified (Figure 2). Among the various three-membered rings considered in this study, the rings **11**, **22**, and **26** are stable relative to the reactant limit (Figure 2).

Rearrangements in *trans*- and *cis*-$H_2C{=}$CHNO. The energized *trans*-nitrosoethylene formed in the reaction of C_2H_3 + NO can undergo any one of the following reactions: (i) cis−trans isomerization, (ii) 1,2-H migration leading to methyl fulminate, **15**, (iii) 1,3-H migration leading to **12**, and (iv) cyclization to give rise to the N-oxide, **11**. We have investigated all these reactions and have identified the transition structures for each of these processes. The most favored unimolecular reaction channel from **1** is the cis−trans isomerization; the cisoid conformation of the conjugated nitrosoalkene is less stable (3.9 kcal/mol), and the magnitude of the isomerization barrier is calculated to be around 8 kcal/mol. Even though methyl fulminate **15** lies energetically below the *trans*-nitrosoethylene, the 1,2-H-migration faces such a high barrier (66 kcal/mol) that the transition structure **1/15** (Figure 6) is disposed energetically above the C_2H_3 + NO limit (Figure 4). The 1,3-H migration to form **12** is slightly endothermic (2.3 kcal/mol) and involves an almost equally high barrier (62.0 kcal/mol). The introduction of the electron-withdrawing nitroso group enhances the electrophilicity of the β carbon atom, which can then form a bond with the lone pair of nitrogen via a 1+2 cycloaddition. The valency of nitrogen has been extended from three to five in this cyclic isomer **11** and because of the ring strain, this isomer is relatively unstable compared to the open-chain isomer. We traced the PES for cyclization and located the transition structure **1/11** (Figure 7). As can be seen from Figure 4, cyclization is a preferred process as compared to 1,2-H and 1,3-H shifts.

The cisoid isomer can further undergo the intramolecular [2+2] cycloaddition reaction, which is characteristic of the α,β-unsaturated nitro compounds. The resulting 1,2-oxazete **3** is nearly isoenergetic with the *cis*-C_2H_3NO isomer, and this process is associated with a barrier height of 33.8 kcal/mol. Ugalde[16a] estimated a barrier height of 49.9 kcal/mol for this path at the MP3/6-31G(d)//HF/6-31G(d) level. Benson[9] assumed this step to be endothermic by about 18 kcal/mol from thermochemical considerations, and in his proposed mechanism for the pyrolysis of acetylene in the presence of nitric oxide, he suggested this step to be the rate-determining step for the termination process in the pyrolytic mechanism. However, as will be discussed later, this step is not the rate-determining step for the HCN formation in the C_2H_3 + NO reaction. The C−N bond distance in **2/3** is smaller than that in **1**, while the N$=$O bond length is longer. In accordance with the Hammond postulate for a thermoneutral reaction, the TS lies more or less in the center of the reaction path. The calculated activation energy is slightly large in comparison with the usual thermal activation energies of 12−24 kcal/mol typical of symmetry-allowed reactions such as conrotatory ring closures. As concluded by Ugalde,[16a] this high barrier could be taken as an indication for the reaction to follow the high energy Möbius aromatic pathway.

The cyclic isomer **11**, once formed, will be in equilibrium with **1** because of the available excess energy. However, this excess energy (25.2 kcal/mol) is not sufficient for its decomposition into C_2H_3 + NO, **31** (E_a = 63.1 kcal/mol). Even though this decomposition reaction plays a less significant role in the kinetics of the title reaction, the transition structure for this reaction is interesting from the theoretical point of view, and its geometry is shown in Figure 7. The eigenvectors of the negative eigenvalue of the force constant matrix (0.69 R_{N-CH_2} − 0.26 R_{C-C} − 0.54 ∠ ONC − 0.23 ∠ CCN) suggest the simultaneous formation of the cyclic C−N bonds. The forming C−N bonds **11/31** are too long (1.66 and 2.28 Å) and the N≡O bond length is close to its value in the isolated NO molecule. The reaction **11** → **31** is an endothermic reaction, and the **11/**

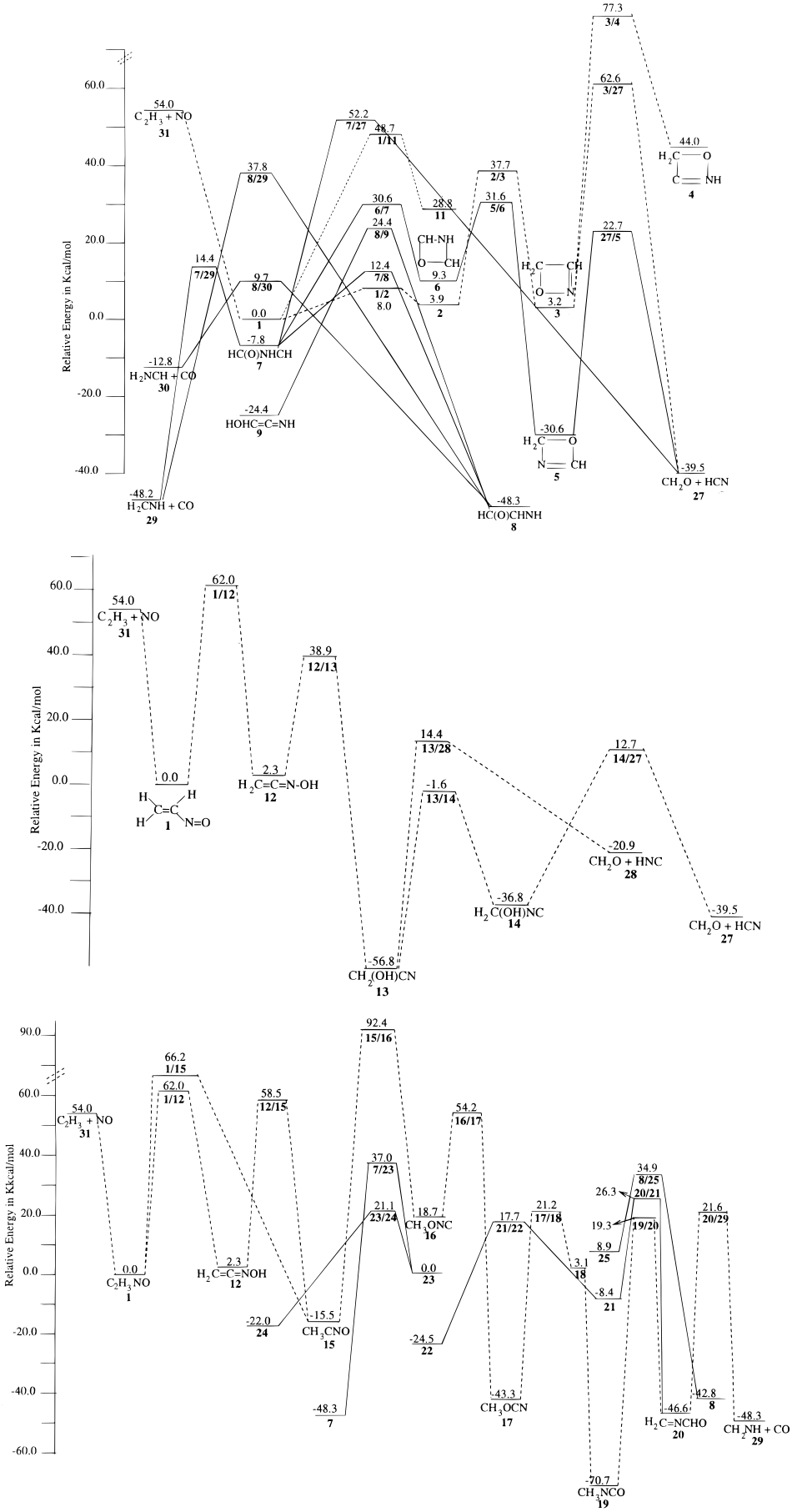

Figure 4. The overall profile of the singlet PES for the [C_2,H_3,N,O] system calculated at MP2/6-311++G(d,p) level. (a) mechanisms **A** and **A′**. Dashed lines correspond to **A** while the solid lines correspond to **A′**. (b) mechanism **B**. (c) mechanisms **C** and **D**. Dashed lines correspond to **C** while solid lines correspond to **D**.

SCHEME 1

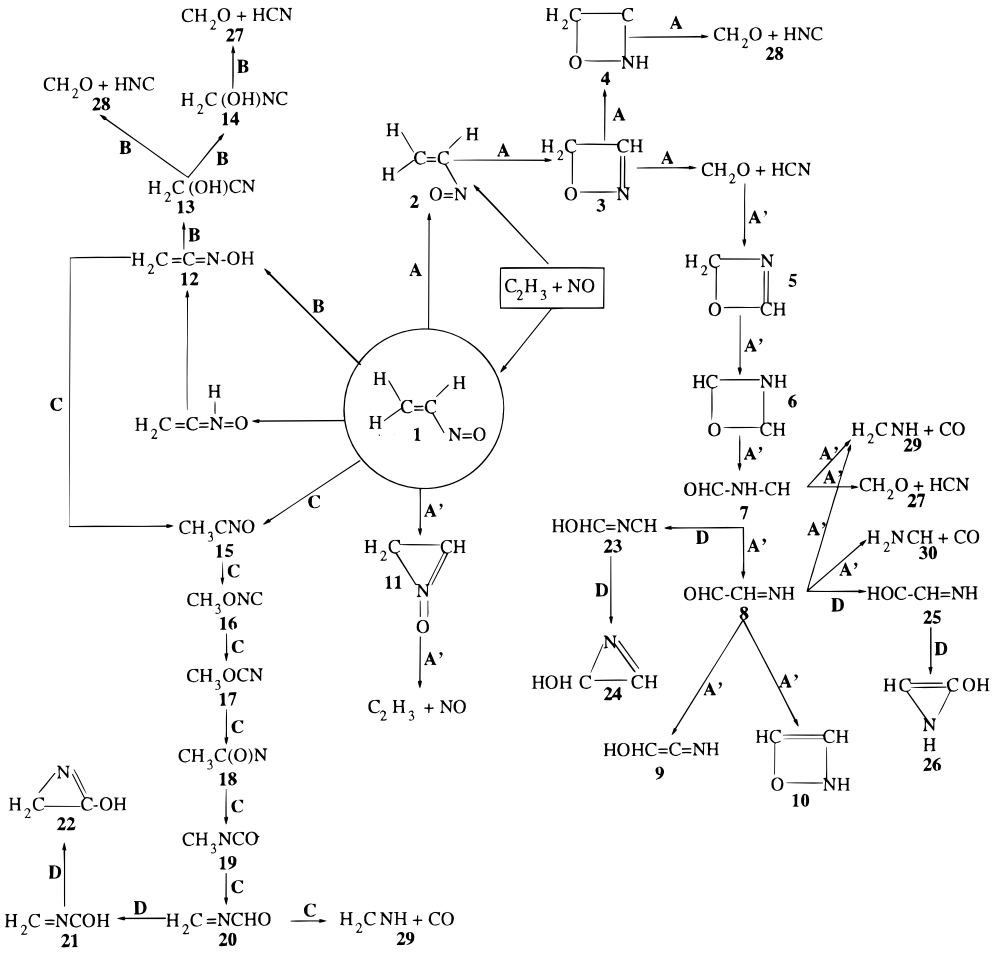

31 geometry is close to **31**, as expected for an endothermic reaction from the Hammond postulate. Similarly, the transition structure for the endothermic cyclization of **1** to **11** has structural parameters close to **11** but very different from **11**/**31**.

Formation of CH_2O + HCN. A quick glance at Scheme 1 reveals that CH_2O formation can occur through various isomers depending upon the entrance channel into the $[C_2H_3NO]$ potential well, and the product distribution will depend heavily upon the available energy of the initially formed adduct. The nascent internal energy distribution of the resulting CH_2O will depend on the mechanism of its formation. The 1,2-oxazete **3** can undergo a pericylic ring opening reaction to form the aldehyde, whose transition structure **3**/**27** (Figure 5) has all four ring atoms lying nearly in the same plane and both the C−C and N−O bonds elongated. If we consider the following pathway (mechanism A) for the formation of CH_2O,

$$C_2H_3 + NO\ \mathbf{31} \rightarrow \mathbf{1} \xrightarrow{1/2} \mathbf{2} \xrightarrow{2/3} \mathbf{3} \xrightarrow{3/27} H_2CO + HCN\ \mathbf{27}$$

the rate-determining step is actually the decomposition of oxazete. This is in contrast to the expectations of Benson[9] but in agreement with the experimental findings of Weiser and Berndt.[20] The latter authors found that the heating of 2-*tert*-butyl-3,3-dimethyl-1-nitroso-1-butene at 220 °C resulted in the oxazete derivative and that a further heating to temperatures above 240 °C resulted in ketone and hydrogen cyanide. Ugalde,[16a] in his calculations at the MP3/6-31G(d) level, reported a barrier height of 73.9 kcal/mol for this step. As is obvious from Figure 4a, the barrier involved in the last step of the above pathway is more than the available excess energy of **3*** and hence at ordinary temperatures, the reaction between vinyl radical and nitric oxide cannot proceed beyond the oxazete formation. This subsequently provides a possible explanation for the nonobservation of CH_2O in the experimental studies of Ogura[8] and Silcocks[2] at lower temperatures.

If we now analyze this reaction from the reverse direction, viz., the [2+2] cycloaddition of H_2CO and HCN, it can proceed in two ways depending upon whether the carbon of the hydrogen cyanide adds on to the carbon or the oxygen end of the aldehyde. As discussed earlier, the product of the latter addition is thermodynamically more stable among the two possible cyclic adducts. Hence, we have searched for the path of the latter addition and identified the corresponding transition structure **27**/**5** (Figure 7). It lies nearly 40 kcal/mol below **3**/**27** and it lies well below the C_2H_3 + NO limit. This result motivated us to further investigate the PES in looking for possible modes of formation of 1,3-oxazete **5** and in turn its unimolecular dissociation channels.

Formaldehyde can also be formed via the 1,2-elimination of HCN from substituted methanols, which in turn can be obtained from **1** via successive 1,3-H and 1,2-OH migrations, as shown in mechanism B (Figure 4b). The rate-determining step in mechanism B is the first step giving rise to the substituted oxime **12**. It should be noticed that the potential energy of the transition structure involved in this step is nearly the same as that for the rate-determining transition structure in mechanism A (Figure 4a). Hence, one should expect a competitive involvement of both the mechanisms. The rearrangement from **12** to cyanomethanol **13** involves two successive 1,2-OH migrations instead of a single 1,3-OH migration. However, we were not

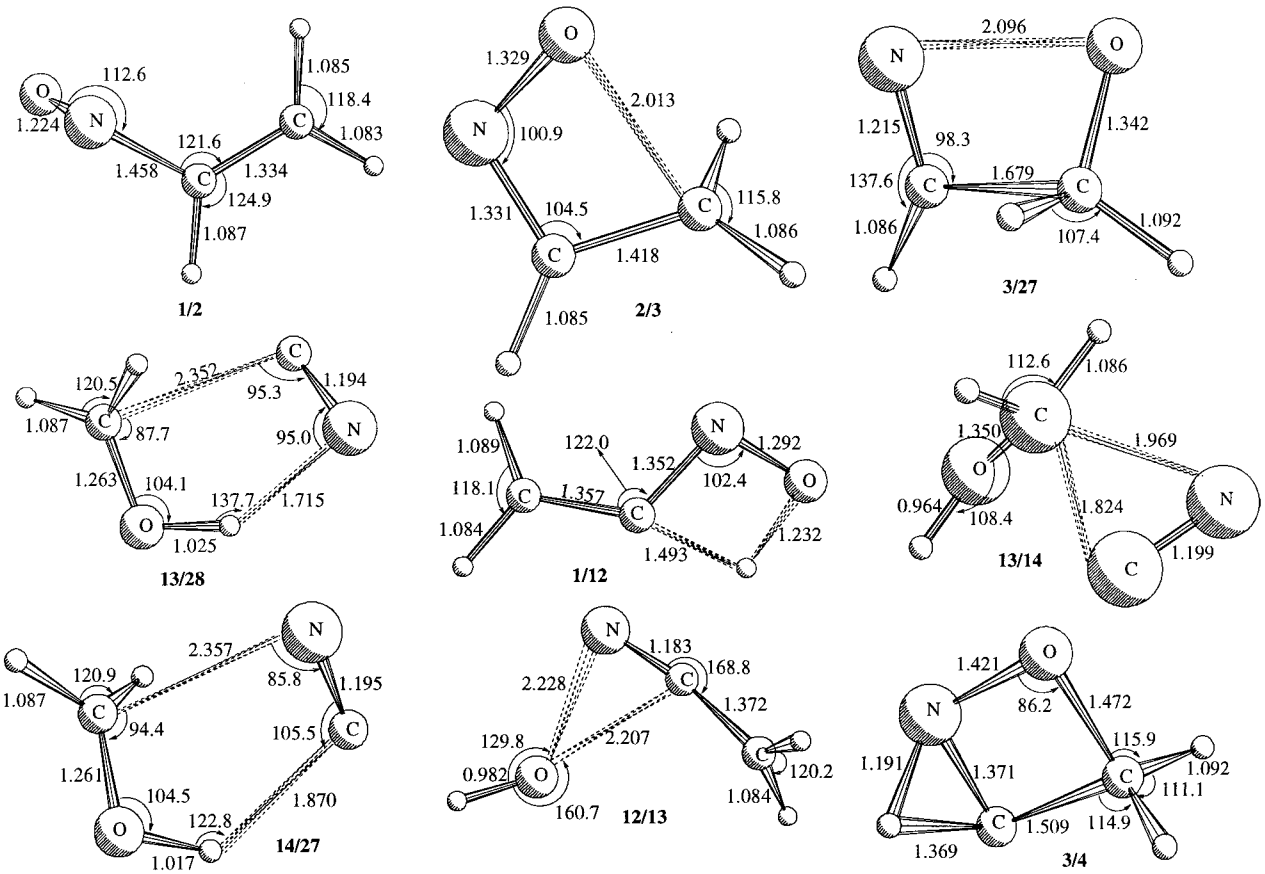

Figure 5. MP2/6-311++G(d,p) optimized geometries of the transition structures involved in mechanisms **A** and **B**. Bond lengths are given in Å and bond angles in degrees.

able to optimize the equilibrium structure of hydroxyvinylnitrene, and all our attempts invariably led to cyanomethanol. Hence, we expect it to be a point of inflection on the PES. The 1,2-elimination of H and CN groups from **13** proceed through a five-membered ring transition structure **13/28**, resulting in the formation of HNC and CH_2O. A second exit channel of cyanomethanol, which is energetically somewhat more favorable, involves isomerization to isocyanomethanol **14**, followed by elimination of HCN via the five-membered transition structure **14/27**. Once the reactants cross the barrier for the initial step in mechanism B, all other steps are energetically feasible and will drive to CH_2O and HCN/HNC products. Thus, in the reaction of vinyl radical with NO, HCN formation occurs competitively via both **A** and **B** mechanisms.

Formation of CO and [CH_3N] Isomers. As stated in the Introduction, the most extensive investigation of NO inhibition on acetylene pyrolysis was done by Ogura,[8] who found HCN and CO in substantial and equal amounts in his experiments. CO can be formed in (i) the initiation reaction

$$C_2H_2 + NO \rightarrow H + CO + HCN$$

or (ii) from the secondary decomposition of the initially formed formaldehyde in the C_2H_3 + NO reaction, or (iii) could be a primary product of the C_2H_3 + NO reaction. We have shown in our earlier work[10] on C_2H_2 + NO that at low temperatures, below 1500 K, NO is not involved in the chain initiation step (in other words, CO cannot be formed through the pathway (i) above). So at lower temperatures, NO radical inhibits the pyrolysis by reacting with the chain carriers such as C_2H_3 and C_4H_3. However, as discussed above, at low temperatures, the inhibition will lead mainly to the nitrosoethylenes **1** and **2**, or less importantly, to oxazete **3** or the cyclic three-membered isomer **11** as the product, and not to CH_2O and HCN. We investigate, therefore, the various primary pathways for the formation of CO in such reactions.

Scheme 1 reveals the likely formation of CO from N-formyl **20** and C-formylformaldimine **8** and formylaminomethylene **7** (Mechanisms C and A′). Formation of N-formylformaldimine **20** from **1*** involves successive 1,2- and 1,3-methyl migrations in the [CNO] chromophore (mechanism **C**), viz., $-CNO \xrightarrow{1,3-} -ONC \xrightarrow{1,2-} -OCN \xrightarrow{1,2-} -C(O)N \xrightarrow{1,2-} -NCO$. In contrast to the preferential 1,2-hydrogen migrations in the [CNO] chromophore in [H,C,N,O] system, 1,3-methyl migrations are preferred in the [C_2,H_3,N,O] system. Due to the bulkiness of the $-CH_3$ group compared to the H atom, cyclic isomers of [CNO] become unstable in the [C_2,H_3,N,O] system. The rate-limiting step in mechanism **C** (Figure 4) is the conversion of the fulminate **15** to isofulminate **16**, the transition structure of which (**15/16**) lies approximately 37.6 kcal/mol above the C_2H_3 + NO limit. This, thereby, limits the primary formation of CO in the C_2H_3 + NO reaction.

N-Formylaminomethylene **7** can be obtained from 1,3-oxazete **5**(mechanism **A′**, see Figure 4a), and once formed can decompose into CO and formaldimine spontaneously. The present results suggest that the [2+2] cycloaddition of CH_2O + HCN will ultimately lead to CO and CH_2NH at higher temperatures via

$$CH_2O + HCN \xrightarrow{5/27} \mathbf{5} \xrightarrow{5/6} \mathbf{6} \xrightarrow{6/7} HC(O)NHCH\ \mathbf{7} \xrightarrow{7/29} CO + CH_2NH$$

As mentioned earlier, we have looked for processes leading

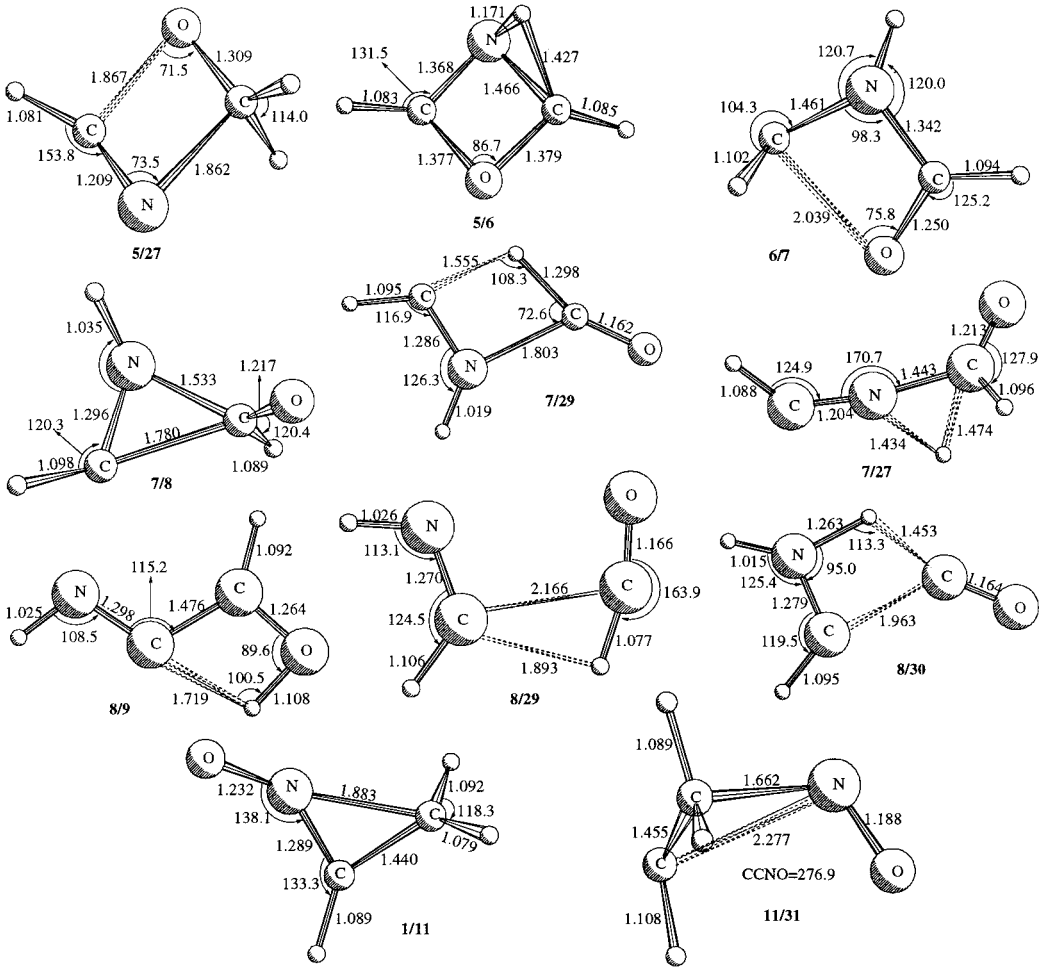

Figure 6. MP2/6-311++G(d,p) optimized geometries of the transition structures involved in mechanisms **C** and **D**. Bond lengths are given in Å and bond angles in degrees.

to the formation of **5** and thereby to mechanism **A′** through some other isomers of $[C_2,H_3,N,O]$. One possible step is the intramolecular [2+2] cycloaddition in N-formylformaldimine

$$CH_2=N-C(O)H\ \mathbf{20}\rightarrow\mathbf{5}$$

We have also investigated this step and identified a transition structure **5/20** at the HF/3-21G level. Our further extensive attempts to obtain the same at MP2/6-311++G(d,p) were not successful. However, as discussed in the beginning of this section, formation of **20** is unfavorable due to the involvement of the **15** → **16** conversion. Hence, in the low-temperature pyrolysis of acetylene in the presence of nitric oxide, NO is likely not involved in the chain initiation step, and NO inhibits the pyrolysis by reacting with the chain carrier, C_2H_3. However, NO inhibition at low temperatures is expected to lead to products other than CH_2O. Furthermore, CO is not a primary product of the inhibiting reaction viz., C_2H_3 + NO. In the experiments of Ogura, HCN and CO are formed in substantial and equal amounts at a rate first-order in both NO and C_2H_2. In the present investigation, we could not find ways to form CO in the same amounts as HCN. Ogura explains his experimental observations by assuming the ethynyl (C_2H) radical to be the chain carrier instead of C_2H_3. It is appropriate to mention our earlier work[21] on the C_2H + NO reaction using the B3LYP/6-311++G(d,p) level of theory, wherein we have identified a pathway for the formation of HCN + CO products without any activation of the initial reactants. However, the formation of the C_2H radical from acetylene and NO (C_2H_2 + NO → C_2H + HNO) is thermochemically indefensible. Therefore, thermochemically feasible pathways for C_2H and CO formation still remain to be investigated.

Concluding Remarks

Electronic structure calculations have been used to characterize the C_2H_3 + NO reaction on its lowest singlet potential energy surface. While some of the equilibrium structures were investigated earlier, we considered nearly all possible isomers and transition states connecting them. While geometries and energies for stationary points on the PES are determined with the MP2 and CCSD(T) levels of theory using the 6-311++G(d,p) basis set, the vibrational frequencies are obtained with a smaller basis set. The main features of the reaction surface are as follows:

(1) A PES consisting of 26 stable intermediates has been characterized, and the relative order of their thermodynamic stability was obtained.

(2) Cis−trans isomerization followed by intramolecular [2+2] cycloaddition is expected to be the favorable unimolecular reaction channel of nitrosoethylenes.

(3) Combination of the reactants C_2H_3 + NO to form C_2H_3-NO occurs without a barrier. Two isomerization pathways are open for the energized adduct **1*** formed from the reactants even at low temperatures, both leading to cyclic adducts (**3** and **11**). However, at low temperatures none of these contain enough energy for subsequent dissociation to products other than C_2H_3 + NO. Therefore, at low temperatures only the adducts **1**, **2**, **3**, and **11** can result, and the C_2H_3 + NO reaction will behave

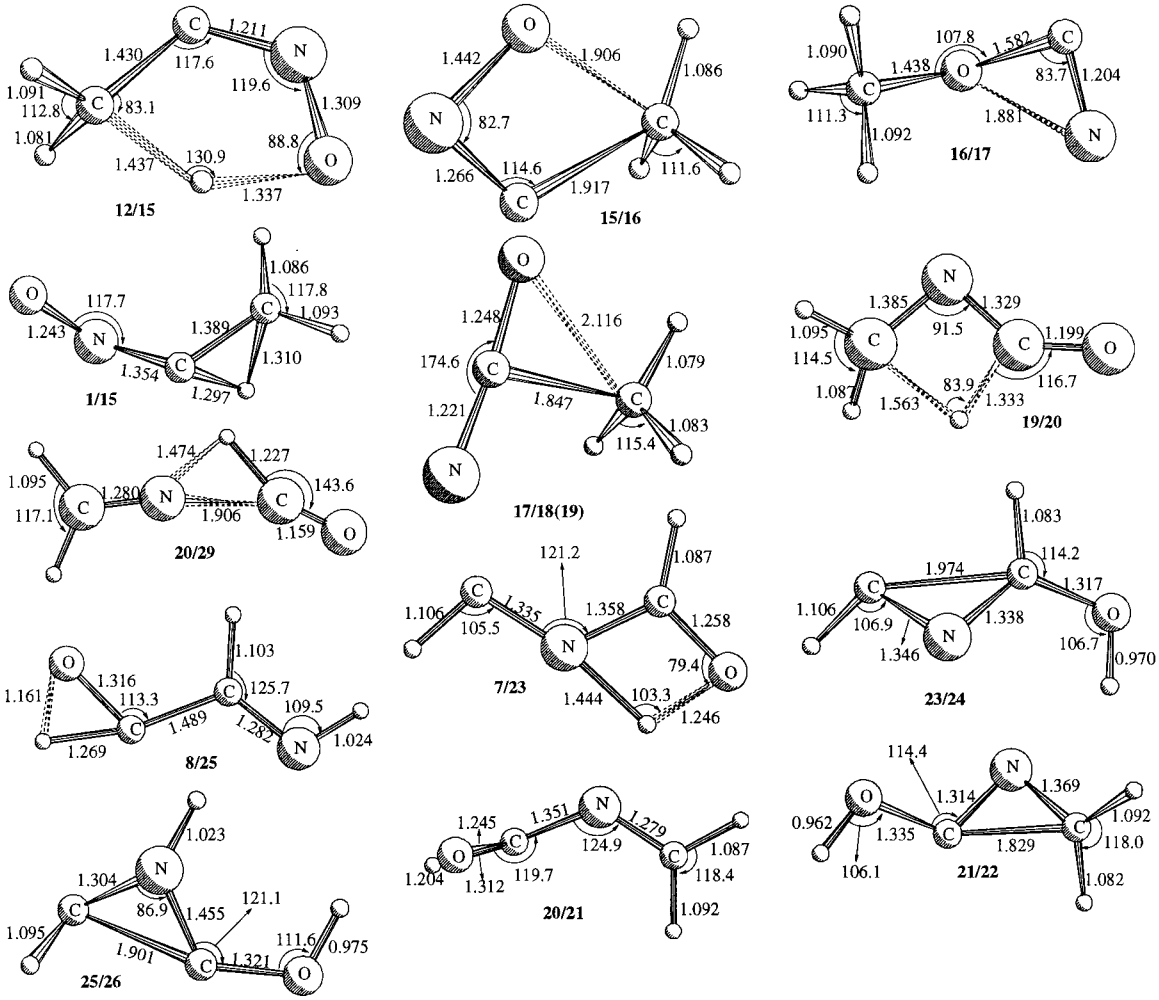

Figure 7. MP2/6-311++G(d,p) optimized geometries of the transition structures involved in mechanism **A′**. Bond lengths are given in Å and bond angles in degrees.

kinetically as a combination reaction, hence becoming fast only at sufficiently high pressures. However, at higher temperatues, the internal energy of the adducts **1**, **2**, and **3** will become high enough for isomerization/dissociation pathways to open (mechanisms A and B) that ultimately result in CH_2O and HCN formation.

(4) Decarbonylation of (**1**) (mechanism **C**), though yielding the thermodynamically more stable product, $CH_2NH + CO$, is kinetically less favorable and therefore expected to contribute only a little toward the total rate.

(5) Of the two possible intermolecular [2+2] cycloaddition products from CH_2O + HCN viz., **3** and **5**, the latter is thermodynamically as well as kinetically favored.

(6) Carbenes and strained three-membered ring isomers do not play any significant role in the reaction kinetics. The existence of a barrier for their cyclization suggests their kinetic stability.

Acknowledgment. H.M.T.N. is grateful to the Flemish Government and the KULeuven Laboratory of Quantum Chemistry for supporting an "Interuniversity Program for Education in Computational Chemistry in Vietnam". R.S. thanks Alexander von Humboldt Stiftung. This work was initiated during an enjoyable stay of M.T.N. at Emory University in 1997 as an Emerson Fellow. He thanks Keiji Morokuma and M.C. Lin for their warm hospitality. We also thank the FWO-Vlaanderen for continuing support.

Supporting Information Available: Unscaled MP2/6-31G** harmonic vibrational frequencies of the stationary points on the PES of $[C_2H_3NO]$ system. Zero-point energies are given in kcal/mol. This information is available free of charge via the Internet at http://pubs.acs.org.

References and Notes

(1) Frank-Kamenetsky, D. A. *Acta Physiochim. USSR* **1943**, *18*, 148. Frank-Kamenetsky, D. A. *J. Phys. Chem. USSR* **1944**, *18*, 329.
(2) Silcocks, C. G. *Proc. R. Soc. London* **1957**, *242A*, 411.
(3) Benson, S. W. *Int. J. Chem. Kinet.* **1992**, *24*, 217.
(4) Palmer, H. B.; Dormish, F. L. *J. Phys. Chem.* **1964**, *6* (8), 1553.
(5) Cullis, C. F.; Franklin, N. H. *Proc. R. Soc. London* **1964**, *280A*, 139.
(6) Minkoff, G. J.; Newitt, D. M.; Rutledge, P. *J. Appl. Chem.* **1952**, *7*, 406.
(7) Minkoff, G. J. *Can. J. Chem.* **1958**, *36*, 131.
(8) (a) Ogura, H. *Bull. Chem. Soc. Jpn.* **1978**, *51*, 3418. (b) Aten, C. F.; Greene, E. F. *Combust. Flame* **1961**, *5*, 55.
(9) Benson, S. W. *Int. J. Chem. Kinet.* **1994**, *26*, 997.
(10) Nguyen, H. M. T.; Nguyen, M. T.; Sumathi, R. *J. Phys. Chem. A* **1999**, *103*, 5015.
(11) Kiefer, J. H. *Int. J. Chem. Kinet.* **1993**, *25*, 215.
(12) (a) Miller, J. A.; Durant, J. L.; Glarborg, P. *27th Symposium (Int.) on Combusion*; Combusion Institute, 1998; p 235. (b) Dagaut, P.; Lecomte, F.; Chevailler, S.; Cathonnet, M. *Combust. Flame* **1999**, in press. (c) Dagaut, P.; Luche, J.; Cathonnet, M. *Combust. Flame* **1999**, submitted.
(13) Sherwood, A. G.; Gunning, H. E. *J. Phys. Chem.* **1965**, *69*, 1732.
(14) Sherwood, A. G.; Gunning, H. E. *J. Am. Chem. Soc.* **1963**, *85*, 3506.
(15) (a) Greenberg, A.; Moore, D. T.; Dubois, T. D. *J. Am. Chem. Soc.* **1996**, *118*, 8658. (b) Pasinszki, T.; Westwood, N. P. D. *J. Phys. Chem.*

1995, *99*, 1649. (c) Shustov, G. V.; Kachanov, A. V.; Chervin, I. I.; Kostyanovsky, R. G.; Rauk, A. *Can. J. Chem.* **1994**, *72*, 279. (d) Mcallister, M. A.; Tidwell, T. T. *J. Chem. Phys.* **1994**, *94*, 2239. (f) Pasinszki, T.; Yamakado, H.; Ohno, K. *J. Phys. Chem.* **1993**, *97*, 12718.

(16) (a) Ugalde, J. M. *J. Mol. Struct. (THEOCHEM)* **1992**, *258*, 167. (b) Arulmozhiraja, S.; Kolandaivel, P. *J. Mol. Struct. (THEOCHEM)* **1998**, *429*, 165.

(17) Frisch, M. J.; Trucks, G. W.; Gordon, M. H.; Gill, P. M. W.; Wong, M. W.; Foresman, J. B.; Johnson, B. G.; Schlegel, H. B.; Robb, M. A.; Replogle, E. S.; Gomperts, R.; Andres, J. L.; Raghavachari, K.; Binkley, J. S.; Gonzalez, C.; Martin, R. J.; Fox, D. J.; Defrees, B. J.; Baker, J.; Stewart, J. J. P.; Pople, J. A. *Gaussian 94*; Gaussian Inc.: Pittsburgh, PA, **1994**.

(18) Mebel, A. M.; Luna, A.; Lin, M. C.; Morokuma, K. *J. Chem. Phys.* **1996**, *105*, 6439.

(19) Kametani, T.; Hibino, S. *Advances in Heterocyclic Chemistry*; Academic Press: New York, 1987; p 42.

(20) Weiser, K.; Berndt, A. *Angew. Chem., Int. Ed. Engl.* **1975**, *14*, 70.

(21) Sengupta, D.; Peeters, J.; Nguyen, M. T. *Chem. Phys. Lett.* **1998**, *283*, 91.